

Implementation of Wavelet Transform-Based Algorithm for Iris Recognition System

Ayra G. Panganiban, Noel B. Linsangan, and Felicito S. Caluyo

Abstract—The purpose of this study is to design a system that will capture the iris image and develop a reliable feature extraction algorithm for iris recognition system. The proposed system is a complete iris recognition system with hardware and software components in which the focus is on the implementation of algorithm based on wavelet transforms. The system consists of the video camera that is interfaced through a frame grabber using the MATLAB program to capture an image of the human eye. The camera includes adjustable chin support, NIR filter and NIR diodes for the lighting and distance settings. The algorithm implemented in software performs segmentation, normalization, feature encoding, and matching. The feature encoding is performed by decomposing the normalized 24 x 240 pixels iris image using Haar and Biorthogonal wavelet families at various levels. The vertical coefficients are encoded into iris templates and stored at the database. The system is evaluated in two modes: verification and identification. The HD values are used as threshold levels to identify the iris image. The number of degrees of freedom is calculated for inter-class comparisons. The test results at different coefficients show that in terms of efficiency, the Haar wavelet decomposition at level 4 is the highest with a Correct Recognition Rate (CRR) of 98% at a feature vector length of 120 bits. The Equal Error Rate (ERR) of the system is 2%. The metrics show that the proposed system provides highly accurate recognition rates and suggest the most appropriate choices that need to be made for best results.

Index Terms—Biometrics, degrees of freedom, hamming distance, iris recognition, wavelet

I. INTRODUCTION

Biometrics plays an important role in high security applications since it uses the unique characteristics of an individual in an electronic system for authentication. Among the existing biometric technologies, it is iris recognition that is considered the most promising. Iris recognition can hardly be forged. Irises have approximately 266 distinctive characteristics, about 173 of which are used to create the iris template [1]. Compared to other biometrics, iris recognition has been around for a shorter period of time. The increasing demand for iris recognition as a security device also demands for the proliferation of its systems, concepts, and algorithms.

The success of iris recognition depends mainly on two factors: image acquisition and iris recognition algorithm [2].

Manuscript received March 15, 2012; revised April 25, 2012.

A. G. Panganiban is with the Computer Engineering Department, Mapua Institute of Technology, Muralla St., Intramuros, Manila, Philippines 1002 (e-mail: agpanganiban@live.mapua.edu.ph).

N. B. Linsangan is the Program Chair of the Computer Engineering Department, Mapua Institute of Technology, Muralla St., Intramuros, Manila, Philippines 1002 (e-mail: nblinsangan@mapua.edu.ph).

F. S. Caluyo is the Dean of the Electrical, Computer and Electronics Engineering, Mapua Institute of Technology, Muralla St., Intramuros, Manila, Philippines 1002 (e-mail: fscaluyo@mapua.edu.ph).

This study implements a system that considers both factors and focuses on the latter. Although many systems had been proposed earlier, many other systems have been developed to satisfy the demand. Huang and Hu [3] declare that at present, the methods proposed by Daugman, Wildes et al., Boles and Boashash are well-known among the existing methods. Daugman uses the multiscale Gabor filters to perform a coarse quantization of the local texture signal, and an iris code computed at 2048 bits. This method is the basis for the present commercial systems. The rights are now owned by the Iridian Technologies company. Wildes et al. have applied the Laplacian pyramid with four different resolution levels to form feature vectors, and used the goodness-of-match based on normalized correlation and Fisher's discriminant for pattern matching. This method is computationally highly demanding. Boles and Boashash used the wavelet transform zero-crossing representation to represent the features of the iris by fine-coarse approximations at different levels, and then the dissimilarity function between two irises was calculated. This algorithm is sensitive to the gray value of an image.

Addison [4] describes a wavelet as a mathematical function used to divide a given function or a continuous-time signal into different frequency components and study each component with a resolution that matches its scale. The wavelets are scaled and they translated copies (known as "daughter wavelets") of a finite-length or fast-decaying oscillating waveform (known as the "mother wavelet"). Wavelet transforms have advantages over traditional Fourier transforms for representing functions that have discontinuities and sharp peaks, and for accurately deconstructing and reconstructing finite, non-periodic and/or non-stationary signals [5]. These underlying characteristics make wavelets applicable for creating the feature vector that is necessary in the iris recognition algorithm.

The central issue on the iris pattern recognition is the relationship of inter-class variability and intra-class variability [6]. This is determined by the degrees-of-freedom which is ideally small for intra-class distribution and large for inter-class distribution. In order to meet the statistical requirements, a representation of images that will create optimal separation among the pattern classes is needed. The standard size of the feature vector used in various studies is 2,048 bits [7], [8] which is not so efficient in terms of storage purposes. Uncompressed image data requires considerable storage capacity and transmission bandwidth. The proliferation of iris recognition systems has not only accelerated the pace of development of many iris image processing software but has also motivated the need for better compression algorithms [9]. While there are existing methods, they however have limitations as stated earlier in

this section, which warrant further study.

The purpose of this study is to design a system that will capture the iris image and develop a reliable algorithm using wavelet coefficients for iris recognition system. The proposed algorithm aims to determine the most efficient wavelet family and its coefficients for encoding the iris template of the experiment samples. This will provide information on how to evaluate the accuracy and efficiency of the wavelet-based iris recognition system. It will also serve as future reference for researchers in the field of the iris recognition.

The system does not involve real-time image processing and matching of iris images of persons with eye disorders. The resolution of the system is limited by the type of camera used. The user can select among the captured iris images and can enroll only the iris feature that is within the range of defined pixels since most iris recognition systems use images with optimal quality in real-time applications. The iris size may vary since the capturing distance from the camera is not strictly controlled and iris images may have a slight rotation due to the variability in the acquisition process. An image must be enrolled first before it can undergo template matching. The speed of the system is also limited by the CPU where the software is deployed. The reliability of the proposed algorithm depends on the Hamming distance values. The performance of the system is evaluated using the number of degrees of freedom (DOF), False Reject Rate (FRR), False Accept Rate (FAR) and Equal Error Rate (EER) [7].

II. DESIGN IMPLEMENTATION

The design of the system involves both the hardware and the software to perform iris image capture and iris recognition and these are illustrated in Fig. 1.

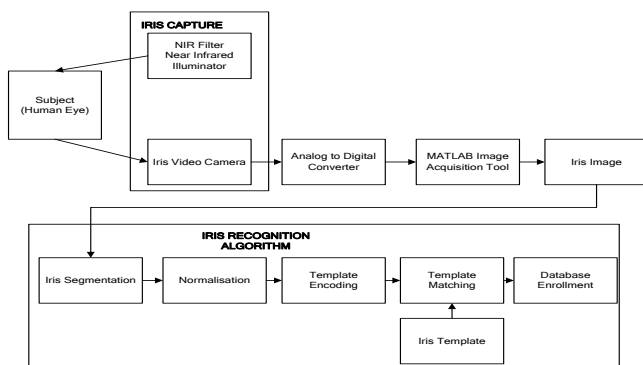


Fig. 1. Block diagram of the Iris Recognition System

A. Hardware Implementation

The hardware is developed using a video camera that captures the texture of the iris image. The camera employs a CCD image sensor. Its focus can be set manually according to user requirement. However, the device alone cannot capture the iris image needed by the proposed software. Lighting and distance to camera were considered to improve image quality. The lighting source is an infrared light. The diodes give off NIR illumination that is not visible to the human eye. Since the lighting condition and camera focus may be varied for different subjects, an adjustable steel bar support is designed for the camera and the infrared light. By this, the user can set

the best distance from the camera and light source to the human eye. A chin support is also integrated in the device to adapt to the user. Since the camera used is analog, an analog-to-digital converter is necessary. In this case, a USB DVD Maker is used to integrate the camera to the PC using the composite video input. The image acquisition toolbox of MATLAB connects the camera to a frame grabber in the system computer. The frames are previewed in the customized graphical user interface to allow the user to select among the most appropriate image settings before enrolling it to the iris recognition software.

B. Software Implementation

1) Pre-processing stage

In the preprocessing stage, the principle is based on the study of Masek [10] where the image is first converted to 8-bit grey scale and reduced to 225 x 300 pixels for faster execution and consistency. The image then undergoes segmentation, normalization and template encoding. The segmentation process is based on the circular Hough transform which defines a circle according to the equation,

$$x^2c + y^2c - r^2 = 0. \quad (1)$$

The Hough transform is a standard computer vision algorithm that can be used to determine the parameters of simple geometric objects such as lines and circles, present in an image [11]. For the captured images, the value of the iris radius ranges from 80 to 150 pixels, while the pupil radius ranges from 20 to 75 pixels. Canny edge detection, a method developed by Canny [12], is employed first to generate an edge map. It uses a multi-stage algorithm to detect a wide range of edges in images. Horizontal lines are drawn for top and bottom eyelid and two circles overlaid for iris and pupil boundaries. The process is able to localize the circular iris and pupil region, occluding eyelids and eyelashes and reflections. Segmentation is highly critical to the success of the iris recognition system [10]. A poor contrast between the iris and pupil and out-of-bound values of iris regions will make segmentation difficult, resulting in poor recognition rates which may be seen in Fig. 2 and 3.

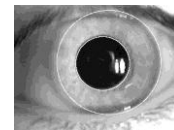


Fig. 2. Successful segmentation.

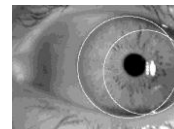


Fig. 3. Failed segmentation.

In order to be able to make comparisons, the segmented iris image should undergo the normalization process. This process transforms the extracted iris region into a rectangular block with constant dimensions to account for imaging inconsistencies which are mainly due to the stretching of the iris from varying levels of illumination. The software uses a technique based on Daugman's rubber sheet model. The centre of the pupil was considered as the reference point, and radial vectors pass through the iris region. A number of data

points are selected along each radial line and this is defined as the radial resolution. The number of radial lines going around the iris region is defined as the angular resolution. A remapping formula is used to rescale points depending on the angle around the circle [10]. For this study, a radial resolution of 24 pixels and an angular resolution of 240 pixels were used. With these settings, the image can be analyzed using 2D wavelets at maximum level of 5.

2) Feature extraction

From the normalized region, a biometric template was created. In this study, the wavelet transform was used to extract the discriminating information in an iris pattern. Two mother wavelets namely Haar and Biorthogonal [5] were experimented on. The image was decomposed using the wavelets at N levels in which level 4 is the maximum. The wavelet transform breaks an image down into four sub-samples or images. The results consist of one image that has been high-pass filtered in the horizontal and vertical directions, one that has been low-pass filtered in the vertical and high-pass filtered in the horizontal, and one that has been low-pass filtered in both directions. Fig 4 illustrates the wavelet decomposition using the MATLAB wavelet toolbox [13].

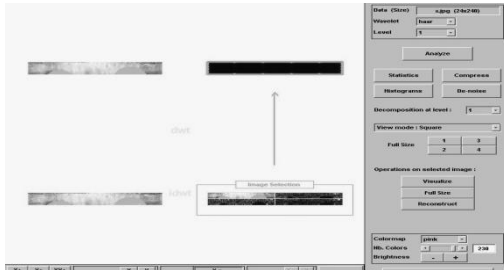


Fig. 4. Wavelet decomposition.

The patterns of small and large squares were predominantly oriented vertically. With this, vertical coefficient is tested to produce the feature vector. Wavelet coefficients at different levels were also considered to find the best feature vector for the system. Each resulting phasor angle in the complex plane is quantized to the quadrant in which it lies at each local element of the iris pattern. The operation is repeated all across the iris. Here, coefficients greater than 0.5 are set to value 11 while coefficients less than 0.5 are set to 10. The feature vector values falling between 0 to -0.5 are set to 01 and those that are smaller than -0.5 are set to 00.

3) Template Storage

The encoded bits are stored in a database using the Microsoft SQL Server for template matching. The database columns consist of an auto-incremented iris identification number, iris image path and iris codes. Table I shows the database model.

TABLE I: DATABASE STRUCTURE

Table Name: IrisDataBank		
Column Name	Data Type	Allow Nulls
Iris_id	int	No
Iris_path	varchar(200)	Yes
Iris_template	varchar(max)	Yes

4) Template Matching

The last stage of the iris recognition software is the template matching. The matching is employed using the

Hamming distance [10] given by the formula,

$$HD = 1/B \sum_{i=1}^B X_i \otimes Y_i \tag{2}$$

where Xi and Yi represent the i-th bit in the sequences X and Y; respectively, and B is the total number of bits in each sequence. The symbol \otimes is the “XOR” operator. To account for possible rotational inconsistencies, the template is bit-wise shifted 8 bits to the left and to the right to obtain multiple Hamming distances, and then the lowest distance is chosen.

5) User-Interface



Fig . 5. User interface of the iris recognition software.

Fig 5 illustrates the graphical user interface developed using the MATLAB GUI builder which contains all the modules for the iris recognition process. The string “Start” shifts to “Stop” and the software starts grabbing frames when the start button is clicked by the user. The image is captured once the stop button is clicked. If the iris image is for enrollment, the enroll button is clicked and the software starts processing the image through the algorithm explained earlier. The template is stored in the database with an identification number. If it is for matching, the Hamming distance is calculated to test whether two iris templates are from the same individual or not.

III. EXPERIMENTAL RESULTS

The performance of the proposed system was evaluated using the common biometric test metrics to determine whether the objectives of the study are met. The reliability of the algorithm was tested in two modes: verification or the test for inter-class relationship and identification or the test for intra-class relationship. Several iris images were taken from fifty (50) individuals. One-hundred (100) datasets were presented in the study for evaluation. For each individual, two (2) iris images from the left eye were taken, one used for enrollment and the other for template matching. A check on the segmentation result was performed all throughout the trials since segmentation is critical to the success of the iris recognition process. The iris images from different individuals whose templates were first stored in the database were used for matching. Each iris image was encoded as a bit pattern to produce the iris template needed in testing the best wavelet coefficient for the study.

Several testing procedures were employed to evaluate the performance of the proposed algorithm. The first test was employed using two-dimensional discrete stationary wavelet analysis. The decomposition was performed using Haar and Biorthogonal wavelet families at various levels. The vertical coefficient was used as template encoding parameter. The calculated Hamming distance values for inter-class and intra-class comparisons are tabulated. The minimum and

maximum Hamming distance values for inter-class comparisons of templates enrolled in the database are identified. Based on statistics, the number of degrees of freedom is the number of values in the final calculation of statistics that is free to vary [15]. In this context, to test the uniqueness of the iris pattern, the number of degrees of freedom represented by the templates was calculated using the formula,

$$DOF = \rho(1 - \rho)/\sigma^2 \quad (3)$$

where ρ is the mean, and σ is the standard deviation of the distribution. The collection of inter-class Hamming distance values approximately follows a binomial distribution.

Table II shows the summary of results. It can be observed that the template encoded using the Biorthogonal family at Level 1 gives the largest number of degrees of freedom. Hence, it is the most effective in separating the classes.

TABLE II: COMPARISON OF NUMBER OF DOF AMONG DIFFERENT FEATURE VECTORS

Mother Wavelet	Level	Feature Vector	DOF
Haar	1	V	41
Haar	4	V	50
Bior1.3	1	V	76
Bior1.3	4	V	69

TABLE III: FALSE ACCEPT RATE AND FALSE REJECT RATE VALUES

Mother wavelet	Level	Coefficient	FAR	FRR
Haar	1	V	0.08	0.03
Haar	4	V	0.02	0.02
Bior1.3	1	V	0.08	0.07
Bior1.3	4	V	0.08	0.03

In order to find out the most efficient wavelet coefficient, the performance of each feature vector was determined in terms of accuracy over vector length or the number of bit patterns. Through the range of Hamming distance values, the threshold values were identified. The Equal Error Rate (EER) values were compared among feature vectors. The Hamming distance values were first classified according to three quality classes based on Quality (Q), namely, Poor (P), Moderate (M) and Good (G). Poor Q means that the Hamming distance value is 10 % lower than the threshold value. Moderate Q means that the user has to decide whether the Hamming distance value agrees with the desired result. This occurs when the value is ± 10 % of the threshold values. Good Q means that the Hamming distance value is 10% higher than the threshold value. First, the False Accept Rate (FAR) and the False Reject Rate (FRR) were measured using 100 samples per coefficient. The Hamming distance values that were classified as M were excluded in the graph since they do not really give concrete decision on template matching. FAR is the probability that the system accepts an unauthorized user or a false template. FRR is the probability that the system rejects an authorized user or a correct template. Table III presents the FAR and FRR values. The results show that no perfect recognition is achieved since there is no instance where FRR and FAR values become 0. However, the FAR of 2% and the FRR of 2% for Haar wavelet decomposed at level 4 give the best results. This suggests that it is the highest in terms of accuracy. These values are presented in graphical

form in Fig 5 to illustrate the Relative Operating Characteristic (ROC) [14]. This shows that the Equal Error Rate of the system is 2%.

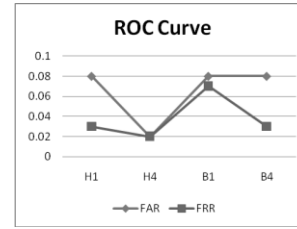


Fig. 5. Relative Operating Characteristic Plot.

The Correct Recognition Rate (CRR) is the probability that the system correctly identifies the input template from the templates in the database [16]. The CRR of the system was evaluated over the vector length to test which among the wavelets has the most efficient feature vector. Table 4 shows that the most efficient vector based on the conducted tests is the Haar wavelet decomposed at Level 4 which has 98% CRR for a 120 feature vector length.

TABLE IV: COMPARISON OF FEATURE VECTOR EFFICIENCY AMONG DIFFERENT MOTHER WAVELETS

Mother wavelet	Level	Feature Vector	Accuracy in %	Feature vector length
Haar	1	V	94.5	480
Haar	4	V	98	120
Bior1.3	1	V	92.5	480
Bior1.3	4	V	94.5	122

IV. CONCLUSION

Based on the results, it can be concluded even though the hardware design is not able to produce an optimal image quality due to constraints on type of camera used, lighting, and distance, the system is still able to capture the images needed by the software for successful recognition. For the proposed algorithm, the results were able to achieve the objectives of this study. Using Haar and Biorthogonal wavelet families at various levels of decomposition, the feature vector was encoded. It was identified that the dominant features of the normalized images were oriented vertically. This is the reason why vertical coefficients were chosen for the implementation rather than the horizontal or diagonal coefficients. The computed number of degrees of freedom based on the mean and the standard deviation of the binomial distribution was able to demonstrate the separation of iris classes. Experimental results show that the Biorthogonal wavelet vertical coefficient at level 4 has the greatest DOF value. The threshold values used in testing was set by observing the minimum value of the inter-class comparison. Hamming distance below the threshold value means that the iris templates come from the same individual. In instances where a clear decision cannot be made based on a preset threshold value, comparisons between the relative values of Hamming distances can lead to correct recognition. Hence, a conclusive determination of identity can be based on both the threshold value and on a comparison of HD values.

Other biometric test metrics provide additional description

of the performance of the system. The FAR and FRR of 2% for Haar wavelet decomposed at level 4 are already acceptable. The results suggest that the Haar wavelet coefficient yield high accuracy and efficiency. The EER of the system is 2%. The Haar wavelet decomposed at Level 4 has 98% CCR for a 120 feature vector length.

REFERENCES

- [1] P. Khaw, *Iris Recognition Technology for Improved Authentication, SANS Security Essentials (GSEC) Practical Assignment*, version 1.3, SANS Institute, 2002, pp. 5-8.
- [2] A. Basit, M. Y. Javed, M. A. Anjum, *Efficient Iris Recognition Method for Human Identification*, World Academy of Science, Engineering and Technology 4, 2005.
- [3] H. Huifang, and H. Guangshu, "Iris Recognition based on Adjustable Scale Wavelet Transform" in *Proc. IEEE*, 2005.
- [4] *The Illustrated Wavelet Transform Handbook*, P. Addison, Institute of Physics, 2002.
- [5] A. Graps, "An Introduction to Wavelets," *IEEE Computational Science and Engineering*, Summer 1995.
- [6] J. Daugman, "Demodulation by Complex-Valued Wavelets for Stochastic Pattern Recognition," *International Journal of Wavelets, Multiresolution and Information Processing*, vol. 1, no.1, pp. 1-17, 2003.
- [7] S. Lim, K. Lee, O. Byeon, and T. Kim. (June 2001). Efficient Iris Recognition through Improvement of Feature Vector and Classifier, *ETRI Journal*, vol 23, no. 2
- [8] J. Daugman, "High Confidence Visual Recognition of Persons by a Test of Statistical Independence," *IEEE Transl. on Pattern Analysis and Machine Intelligence*, vol. 15, issue 11, 1993.
- [9] T. Yew, "Detail Preserving Image Compression using Wavelet Transform," *IEEE Region Student Paper Contest UG Category*, 1995.
- [10] L. Masek, "Recognition of Human Iris Patterns for Biometric Identification", Ph.D. dissertation, The University of Western California, 2003.
- [11] Shapiro, Linda, and G. Stockman, *Computer Vision*, Prentice-Hall, Inc., 2001.
- [12] J. Canny, "A Computational Approach To Edge Detection," *IEEE Trans. Pattern Analysis and Machine Intelligence*, 8:679-714, 1986.
- [13] *Wavelet Toolbox 4 User's Guide*, M. Misiti, Y. Misiti, G. Oppenheim, and J Poggi, 1997-2009.
- [14] R.P. Wildes, "Iris Recognition: An Emerging Biometric Technology," in *IEEE Proc.*, vol. 85, issue 9, 1997.
- [15] J. Daugman, "How Iris Recognition Works" in *IEEE Proc. on Image Processing*, 2002, pp. 33-36, doi: 10.1109/ICIP.2002.1037952.
- [16] S. Attarchi, K. Faez, and A. Asghari, "A Fast and Accurate Iris Recognition Method Using the Complex Inversion Map and 2DPCA" in *IEEE Conference on Computer and Information Science*, May 2008, pp. 179-184, doi:10.1109/ICIS.2008.69.